

Chapter 1: Highlights from Virgo

Gravitational Waves (GW) give fundamental informations on the Universe. By comparing the four fundamental nature's interaction constants we realize that gravitational interaction is 34 order of magnitude smaller than the other:

Strong	Electromagnetic	Weak	Gravitational
$\alpha_s=1$	$e^2=1/137$	$G_F M^2=10^{-5}$	$G_N M^2=10^{-39}$

where M is the proton mass and we have set Planck's constant and light speed equal to 1.

This smallness has as a consequence that gravitons escape undisturbed when other particles interact many times; this happens in supernovae collaps where neutrinos undergoes about 1000 interactions before escaping and gravitons none.

This peculiarity makes that gravitons decouples from Big-Bang hot matter after 10^{-43} s, the Planck's time, corresponding to $\sim 10^{18}$ TeV. Graviton detection seems the only way to reach times closed to 10^{-23} s (because we are sensitive only to the "acoustic" band of frequencies) for studying Big-Bang.

The existence of Gravitational Waves

Einstein's General Relativity Theory¹ (GTR) has as a consequence the existence² of GW; this has been demonstrated by Taylor and Hulse³ by observing for about 20 years the neutron stars binary system PSR 1913+16. They demonstrated that the binary system energy loss follows at 1/1000 level the GTR predictions:

$$\dot{P}_{MEAS} / \dot{P}_{GTR} = 1.0023 \pm 0.0047$$

Where P_{MEAS} and P_{GTR} are the revolution periods measured and predicted by GTR respectively. This measure give a non contradicted evidence of GW existance.

GW-Mass interaction, polarization effects and the GW transmitter

Gravitational Waves are a consequence of Einstein's General Relativity; they are shown to be ripples in the space-time curvature traveling at light speed. In curved space-time the invariant distance ds between two neighbouring events is described by Metric Tensor $g_{\mu\nu}$:

$$\begin{cases} ds^2 = g_{\mu\nu} dx^\mu dx^\nu \\ g_{\mu\nu} g^{\nu\lambda} = \delta_\mu^\lambda \end{cases} \quad \text{In Flat Space} \quad g_{\mu\nu} \Rightarrow \eta_{\mu\nu} = \begin{pmatrix} 1 & 0 & 0 & 0 \\ 0 & -1 & 0 & 0 \\ 0 & 0 & -1 & 0 \\ 0 & 0 & 0 & -1 \end{pmatrix}$$

The evolution of the metric tensor is given by Einstein's equations:

$g_i^k R_{k\mu\nu}^i = R_{\mu\nu} = \frac{8\pi G}{c^4} \left(T_{\mu\nu} - \frac{1}{2} g_{\mu\nu} g_i^l T_l^i \right)$ $R_{klm}^i = \frac{\partial \Gamma_{km}^i}{\partial x^l} - \frac{\partial \Gamma_{kl}^i}{\partial x^m} + \Gamma_{nl}^i \Gamma_{km}^n - \Gamma_{nm}^i \Gamma_{kl}^n$ $\Gamma_{kl}^i = \frac{1}{2} g^{im} \left(\frac{\partial g_{mk}}{\partial x^l} + \frac{\partial g_{ml}}{\partial x^k} - \frac{\partial g_{kl}}{\partial x^m} \right)$	<p>Einstein Eq.</p> <p>Riemann Tensor</p> <p>Christoffel Symbols</p>
---	---

Where $T_{\mu\nu}$ is the energy-momentum tensor and G is Newton's constant .
 The presence of Momentum-Energy tensor $T_{\mu\nu} \neq 0$ changes $\eta_{\mu\nu}$ in $g_{\mu\nu}$ according to Einstein's equations. When gravity is "small" we may write $g_{\mu\nu} = \eta_{\mu\nu} + h_{\mu\nu}$, where $h_{\mu\nu}$ is infinitesimal; to first order in $h_{\mu\nu}$ Einstein equation becomes:

$\square \Psi_{\mu\nu} = (8\pi G/c^4) \tau_{\mu\nu}$	$\Psi_{\mu\nu} = h_{\mu\nu} - \frac{1}{2} \delta_{\mu\nu} h_\lambda^\lambda$
--	--

and $\tau_{\mu\nu}$ is $T_{\mu\nu}$ expanded to first order in $h_{\mu\nu}$. From momentum-energy conservation

$$\partial_\mu \tau_{\eta\nu} = 0$$

and considering that $\tau_{00} = \rho c^2$, where ρ is the matter density, it follows:

$$\Psi_{\alpha\beta} = -\frac{2G}{c^4 R_0} \left(\frac{\partial^2}{\partial t^2} \int \rho x_\alpha x_\beta dV \right)_{t-R_0/c}$$

where R_0 is the source distance and ρ source mass density.
 $\Psi_{\mu\nu}$ has 16 el. , Symmetry reduces to 10, Gauge transf. $x' = x + \epsilon$ ($\square \epsilon = 0$) reduces to 6, Transversality and Tracelessness (TTsystem) reduces to 2:

$h_{\mu\nu}^{TT} = h_{11}^{TT} \begin{pmatrix} 0 & 0 & 0 & 0 \\ 0 & 1 & 0 & 0 \\ 0 & 0 & -1 & 0 \\ 0 & 0 & 0 & 0 \end{pmatrix} + h_{12}^{TT} \begin{pmatrix} 0 & 0 & 0 & 0 \\ 0 & 0 & 1 & 0 \\ 0 & 1 & 0 & 0 \\ 0 & 0 & 0 & 0 \end{pmatrix} = h^+ e_{ik}^+ + h^x e_{ik}^x$	<p>GW along X_3</p>
--	---

It is easy now to show that GW have spin 2 because a 45 degree rotation exchange h^+ with h^x and viceversa.

The Riemann tensor in the TT gauge reaches its simplest form:

$R_{iklm} \Rightarrow R_{0\alpha 0\beta} = -\frac{1}{2} \ddot{h}_{\alpha\beta}^{TT}$	<p>where $\ddot{h}_{\alpha\beta}^{TT} = -\frac{2G}{c^4 R_0} \left(\frac{\partial^2}{\partial t^2} \int \rho (x_\alpha x_\beta)^{TT} dV \right)_{t-R_0/c}$</p>
--	---

i.e. in the limit of weak gravity, GW amplitude is proportional to the second time derivative of the mass quadrupole moment. This is the GW Transmitter.

The GW receiver

A particle moving freely under the action of a gravitational field has its x^μ coordinate satisfying the geodesic equation:

$$\boxed{\frac{d^2 x^\mu}{d\tau^2} = \Gamma_{\alpha\beta}^\mu \frac{dx^\alpha}{d\tau} \frac{dx^\beta}{d\tau}}$$

Where τ is the proper time; It is always possible to find a space-time trajectory in which $\Gamma^\mu_{\nu\lambda}=0$ at any time; along this trajectory a particle is freely falling. Let's consider two freely falling particles A and B (see Fig. 1), their separation $\xi^\alpha = (x_A - x_B)^\alpha$ satisfies the geodesic deviation equation:

$$\boxed{\frac{D^2 \xi^\alpha}{d\tau^2} + R^\alpha_{\beta\gamma\delta} \xi^\gamma \frac{dx^\beta}{d\tau} \frac{dx^\delta}{d\tau} = 0}$$

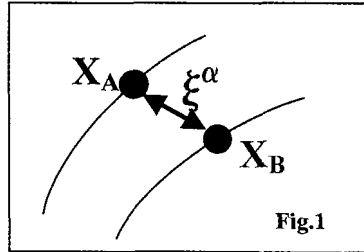


Fig.1

D^2 is the second covariant derivative:

With the purpose of evaluating ξ^α let's put $x^A=0$ in the A particle CMS, x^A_0 equal to proper time

$$\boxed{\frac{D^2 \xi^\alpha}{d\tau^2} = \frac{d^2 \xi^\alpha}{d\tau^2} + \frac{d\Gamma^\alpha_{\beta\mu}}{d\tau} \xi^\beta \frac{dx^\mu}{d\tau} + \Gamma^\alpha_{\beta\mu} \frac{d}{d\tau} (\xi^\beta \frac{dx^\mu}{d\tau}) + \Gamma^\alpha_{\beta\mu} (\frac{d\xi^\beta}{d\tau} + \Gamma^\beta_{\epsilon\nu} \xi^\epsilon \frac{dx^\nu}{d\tau}) \frac{dx^\mu}{d\tau}}$$

τ and the coordinate axis connected to gyroscopes carried by A. At $x^A=0$ since A is freely falling along the geodesic line, we can obtain $(\Gamma^\mu_{\nu\lambda})_{x=0}=0$, $(d\Gamma^\mu_{\nu\lambda}/d\tau)_{x=0}=0$, consequently:

$$\boxed{\frac{D^2 \xi^\alpha}{d\tau^2} = \frac{d^2 \xi^\alpha}{d\tau^2} = -R^\alpha_{\beta\gamma\delta} \xi^\gamma \frac{dx^\beta}{d\tau} \frac{dx^\delta}{d\tau}}$$

To first order in $h^{TT}_{\mu\nu}$, since the only surviving terms are for $\beta = \delta=0$ and $\tau = t$, and remembering that

$$\boxed{R_{0\alpha 0\beta} = -\frac{1}{2} \ddot{h}_{\alpha\beta}^{TT}}$$

it follows that the relative acceleration of B with respect A is:

$$\boxed{\frac{d^2 \xi^\alpha}{d\tau^2} = \frac{1}{2} \ddot{h}_{\alpha\beta}^{TT} \xi^\beta}$$

and the Riemann force is

$$F_\alpha = \frac{1}{2} M \ddot{h}_{\alpha\beta} \xi^\beta$$

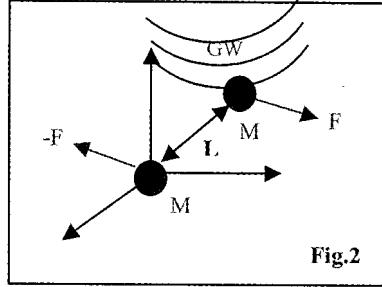
Consequently the receiver is a device measuring space-time curvature i.e. the relative acceleration of two freely falling masses or their relative displacement.

GW produce real tidal accelerations on the bodies embedded in space-time; considering the reference system shown in fig.2, the two masses M will undergo a relative acceleration A_β and the Riemann force F.

$$A_\beta = -\frac{1}{2} L_\alpha \frac{d^2}{dt^2} h_\beta^\alpha$$

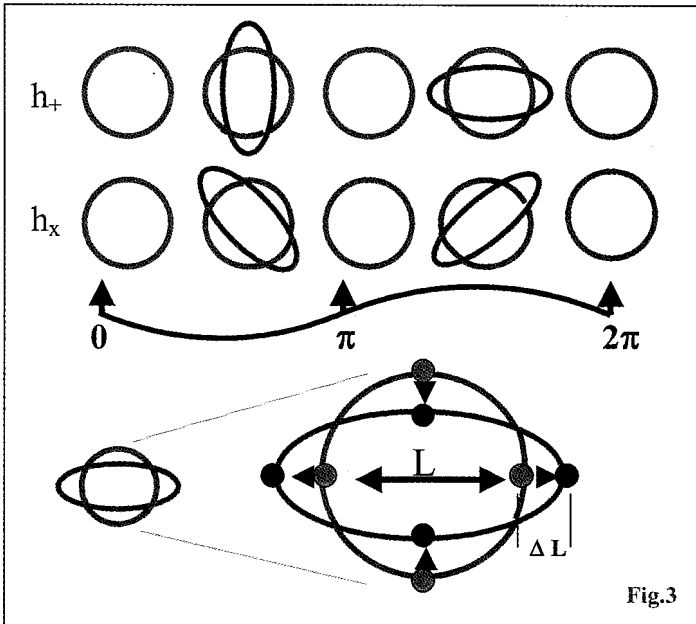
$$F_\beta = M A_\beta$$

(1)



where L_α is the mass separation. This equation is valid in the limit $\lambda \gg L$ and in this limit we note that Riemann force increases with L.

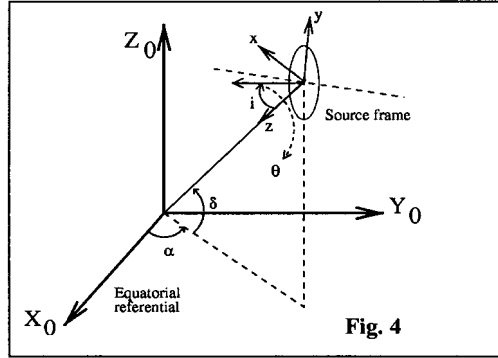
GW have two state of polarization h_+ and h_x ; the effect on a massive ring whose plain is perpendicular to wave propagation direction, is to produce a deformation as shown in fig.3.



Short outline about GW sources

Coalescing binaries

These systems are formed by two compact stars, neutron stars and black-holes, rotating one around the other. In fig.4 the reference system for a coalescing binaries system having with respect to the equatorial system (X_0, Y_0, Z_0) , direction (α, δ) and angles (i, θ) of the orbit plane normal with respect to the direction (α, δ) .



The detector responds to the GW action in the following way:

$$h(t) = h_+(t) F_+(\alpha, \delta) + h_x(t) F_x(\alpha, \delta) \quad (2)$$

Where F_+ and F_x depend from detector orientation and h_+ and h_x are given by:

$$\begin{pmatrix} h_+ \\ h_x \end{pmatrix} = 2.6 \times 10^{-21} \left[\frac{1 \text{ Mpc}}{D} \right] \left[\frac{\mu^{3/5} M^{2/5}}{M_\odot} \right]^{5/3} \left[\frac{v(t)}{100 \text{ Hz}} \right]^{2/3} \times \begin{pmatrix} \cos \Phi(t) \frac{\cos^2 i + 1}{2} \cos(2\theta) + \sin \Phi(t) \cos i \sin 2\theta \\ \sin \Phi(t) \cos i \cos(2\theta) - \cos \Phi(t) \frac{\cos^2 i + 1}{2} \sin(2\theta) \end{pmatrix} \quad (3)$$

Where $\mu = M_1 M_2 / (M_1 + M_2)$ is the reduced mass and $M = M_1 + M_2$ is the total mass, M_\odot is the Sun mass and Φ is:

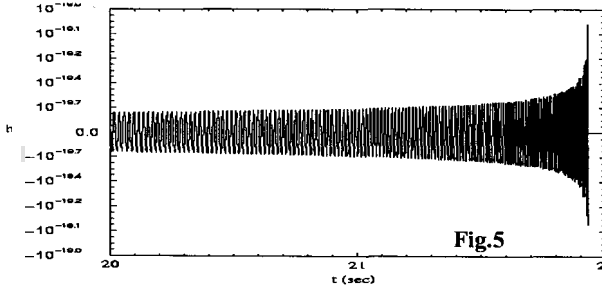
$$\Phi(t) = \Phi_0 + \int_0^t v(\tau) d\tau \quad (4)$$

The frequency as a time function is given by:

$$v(t) = \frac{1}{\pi} \left(\frac{5}{256} \frac{1}{K^{5/3}} \frac{1}{(t-t_0)} \right)^{3/8} \quad (5)$$

Where $K=(\mu M^{2/3})^{3/5}$ is the Chirp Mass and t_0 the coalescence time.

The typical received signal will have a shape similar to the one shown in fig.5; on the last ms strong GRT nonlinearities will occur.



The signal Fourier transform $h(\nu)$ is given by:

$$h(\nu) \propto \nu^{-7/6} e^{i\Phi(K, \dots)} \tag{6}$$

The signal analysis consists in filtering the detector signal with a series of templates in which the unknown parameters M, μ , the initial phase.... are cyclically explored by means of Wiener integrals:

$$\frac{s}{n} = \int d\nu \frac{\text{Re}(S+h)V_n^*}{S^2} e^{i\omega t} \tag{7}$$

Where S is the spectral noise and $S+h$ is the detector signal+ noise, V_n is the n -th template and t the arrival time.

The expected rate is some event per year in a 50Mpc sphere.

Supernovae (SN)

The theoretical evaluation of GW emission from SN explosions has a large uncertainty since the fraction of energy converted in GW is uncertain too; it is assumed a fraction between 10^{-6} and 10^{-3} . The expected rate is about 1/30 years in our Galaxy with $h \sim 10^{-20}$ and about 1/year in the Virgo cluster with $h \sim 10^{-23}$.

Periodic Sources

In our Galaxy are about 10^9 - 10^{10} Neutron Stars (NS) which may emit because of some mass distribution asymmetry both at the rotation and twice the rotation frequency ν .

Since Earth rotates both around the Sun and around his polar axis, the detector receives a non-monochromatic signal because of Doppler shift:

$$e^{i\omega t} \Rightarrow e^{i\omega(t - \vec{n} \cdot \vec{R}/c)} \tag{8}$$

where \bar{n} is the NS direction, $\omega=2\pi\nu$ and \bar{R} is the vector connecting the detector to the cms of the Sun-Earth system. The Doppler shift widens the relative natural frequency width $\Delta\nu=1/T$, where T is the observation time, to $\Delta\nu/\nu\sim 10^{-4}$. For eliminating this effect we need to know ω and \bar{n} and this happens only for known Pulsars.

The known Pulsars are about 1400 and those in the Virgo bandwidth, above 4 Hz, about 700.

If ω and \bar{n} are unknown the optimal analysis method is the "blind search" consisting in dividing the space (ω , \bar{n}) in cells and evaluate (ω_i, \bar{n}_i) in each cell and compute the FFT

of the data multiplied by $e^{+i\omega, \bar{n}, \bullet \bar{R}/c}$ the FFT will be repeated in every cell and the

sky will be explored till a high S/N ratio is found.

The payed price is enormous because for obtaining the maximal frequency resolution $\Delta\nu=1/T$ we need about 10^{22} sky cells; consequently the computing power required becomes impossibly large hence hierarchical methods are under study.

Cosmological BKG^{4,5}

Perhaps the most important signal to search for; it gives informations on the Big-Bang at time close to Planck time. For being detected it requires coincidence between two close high sensitivity interferometers.

Mass displacement due to GW action.

As shown in Fig. 6, GW produce a mass displacement; this displacement, ΔL , is extremely small and may be optimistically evaluated to be in the order $\Delta L \sim 10^{-22}L$.

Thermal noise, created by mirror and mirror suspension wires atom, is the dominant noise at room temperature. To detect GW the thermal stockastic force¹³ should be smaller than the one produced by GW:

$$\frac{1}{2}M\omega^2L_\alpha h_\beta^\alpha > \sqrt{\frac{4kTM\omega_0^2}{Q\omega} \frac{N}{\sqrt{Hz}}}$$

Where M is the oscillator's mass, Q his quality factor, $\nu_0=\omega_0/2\pi$ the resonance frequency and T the temperature.

By defining the spectral GW amplitude as $\tilde{h}_\beta^\alpha (1/\sqrt{Hz})$ and defining, $L_\alpha \tilde{h}_\beta^\alpha = L \tilde{h}$

The measurability condition becomes

$$\tilde{h} > \frac{2}{L\omega^2} \sqrt{\frac{4kT\omega_0^2}{MQ\omega} \frac{1}{\sqrt{Hz}}}$$

From this condition detector topology is following:

-If L is small (some meter) and the source has Fourier components around 1000Hz, the Bar crygenic^{6,7,8,9,10} detectors working at very low temperature (1K) are needed.

-If L is large (some km) it is possible to have high sensitivity at low frequency too (some Hz) and the detector may work at room temperature (but at low temperature seems even better); this is the working condition for **Interferometric detectors**¹¹.

In the following we will concentrate our attention on the Virgo interferometric detector.

Interferometers as GW detector

Eq. 1 gives the relative acceleration, due to GW interaction, of two freely falling objects separated by the distance L .

We should find out the effect of interferometric measurement of masses distance. For doing this evaluation let's observe test masses displacement in a system in which they are at rest.

From General Relativity Theory it follows that if we change reference system by ε_μ also $h_{\mu\nu}$ changes according to a transformation, which leaves invariant ds^2 :

$$\left\{ \begin{array}{l} x'_\mu = x_\mu + \varepsilon_\mu \\ h'_{\mu\nu} = h_{\mu\nu} - \frac{\partial \varepsilon_\mu}{\partial x_\nu} - \frac{\partial \varepsilon_\nu}{\partial x_\mu} \end{array} \right.$$

It is then possible to find the appropriate ε_μ in such a way that mirror separation does not varies; in this new reference system the perturbed photon ds^2 is:

$$ds^2 = c^2 dt^2 - (1 + h_{11}^{TT}) dx^2 - (1 + h_{22}^{TT}) dy^2 = 0$$

where $h_{11}^{TT} = -h_{22}^{TT} = h(t) = h \cos(\Omega_g t + \varphi)$; integrating we obtain, for a ray traveling along x axis and scattered back by a mirror at distance $x=L$, the round trip retarded time t_r :

$$\begin{aligned} c dt \left(1 - \frac{1}{2} h \cos(\Omega_g t + \varphi) \right) &= dx \\ c(t_r - t) - \frac{1}{2} h \frac{\sin(\Omega_g t_r + \varphi) - \sin(\Omega_g t + \varphi)}{\Omega_g} &= -2L \end{aligned}$$

To first order in h we obtain:

$$\begin{aligned} c(t_r - t) - \frac{1}{2} h_\pm \frac{\sin(\Omega_g(t - \frac{2L}{c}) + \varphi) - \sin(\Omega_g t + \varphi)}{\Omega_g} &= -2L \\ t_r &= t - \frac{2L}{c} - \varepsilon h_\pm \frac{L}{c} \frac{\sin \eta}{\eta} \cos(\Phi - \eta) \end{aligned}$$

Where $\eta = \Omega_g L/c$ and $\varepsilon = \pm 1$ if the photon is traveling along x or y axis respectively. The time dependent part of the EM fields along the trajectory, after a round trip $2L$ long, is:

$$A(t) = A_0 e^{-i\omega\left(t - \frac{2L}{c} - \frac{L \sin \eta}{c} \cos(\Phi - \eta)\right)} \sim A_0 e^{-i\omega\left(t - \frac{2L}{c}\right)} \left(1 + i\omega \varepsilon h \frac{L \sin \eta}{c} \cos(\Phi - \eta)\right)$$

For F round trips in a Fabry-Perot cavity we obtain¹¹ the phase shift produced by GW:

$$\varphi(t) = \frac{\omega h F L}{c \sqrt{1 + (F \Omega_g L / c)^2}} \quad \text{cutoff freq. } \nu_g = \frac{c}{2\pi F L}$$

We see that the cavity has a storage time $F L / c$ acts as a low pass filter ; above that cutoff frequency the cavity starts losing sensitivity. A typical value $\nu_g = 1 \text{ kHz}$ is set for being maximally sensitive to supernova explosions events whose characteristic GW emission time is $\approx 1 \text{ ms}$.

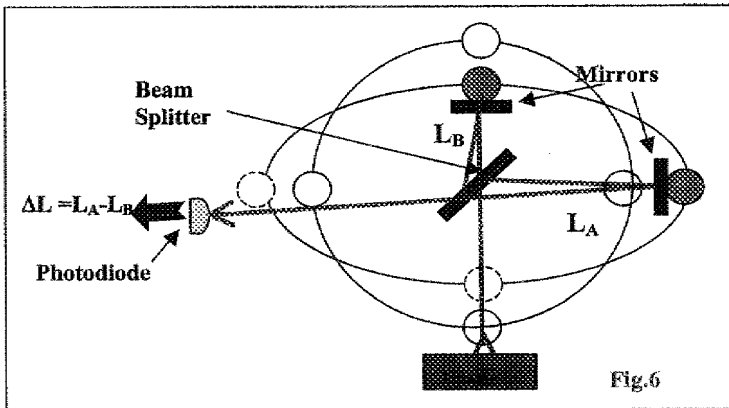
The Virgo Collaboration

Virgo is a french-italian collaboration between CNRS and INFN. The following groups are involved: Lapp (IN2P3 Annecy), OCA (CNRS Nice), SMA (IN2P3 Lyon), Orsay(IN2P3 Orsay), ESPCI (CNRS Paris) on the french side and the italian INFN groups of Firenze-Urbino, LNF, Perugia, Pisa, Roma1, Napoli.

The collaboration is composed by about 100 physicists and a similar number of technicians. Virgo is built at S. Stefano a Macerata locality, about 15 km from Pisa.

The typical diagram of Virgo interferometric detector

In Fig.7 the typical scheme for the interferometric read out system of test mass displacement is shown¹²; since the GW changes L_A and L_B in different way, the measurement of $\Delta L = L_A - L_B \neq 0$ gives a GW amplitude measurement.



The interferometric measurement sensitivity may reach $\sim 10^{-19}\text{-}10^{-20}$ m/Hz^{1/2} hence for measuring $\Delta L/L \sim 10^{-22}$ at room temperature, L_A and L_B should be Km long. The large interferometer arm length and frequency band are enumerated in table 1.

Table 1

Italy	VIRGO	Cascina	3km	4-10000 Hz
USA	LIGO	Hanford	4km	70-10000 Hz
USA	LIGO	Hanford	2km	70-10000 Hz
USA	LIGO	Louisiana	4km	70-10000 Hz
Ge-GB	GEO	Hannover	600m	70-10000 Hz
Japan	TAMA	Tokyo	300m	100-10000 Hz

In fig. 8 the typical optical scheme of Virgo and LIGO like detectors is shown: in Virgo a laser NdYAG having ~ 20 w is prestabilized by a Fabry-Perot (FP) triangular rigid cavity 30 cm long to spectral frequency width $\sim 10^{-2}$ Hz/Hz^{1/2} @10 Hz. The prestabilized laser is then injected in a FP triangular cavity 144 m long in such a way of filtering out all the transvers modes and leaving only the TEM₀₀. The beam then traverse the Recycling Mirror (RM) and enters through the Beam Splitter (BS) mirror which split it into Nord and West beams. The two beams then enter the two FP cavities where about 50 reflections occur for a total of 150 km. Subsequently the photons reach the BS mirror and the phase can be varied in such a way that all the power flows toward RM and the sidebands, containing the signal, flows through a mode cleaner, to the photodiodes. The beam sent to RM is then sent toward BS by RM and the power at BS increased by a factor ~ 50 with the purpose of reducing shot noise. The RM effect is not only to reduce shot noise but also to stabilize laser frequency at level of 10^{-6} Hz/Hz^{1/2} @10 Hz. This spectral frequency width reduction is vital since FP arms might have storage time asymmetries as large as 10%.

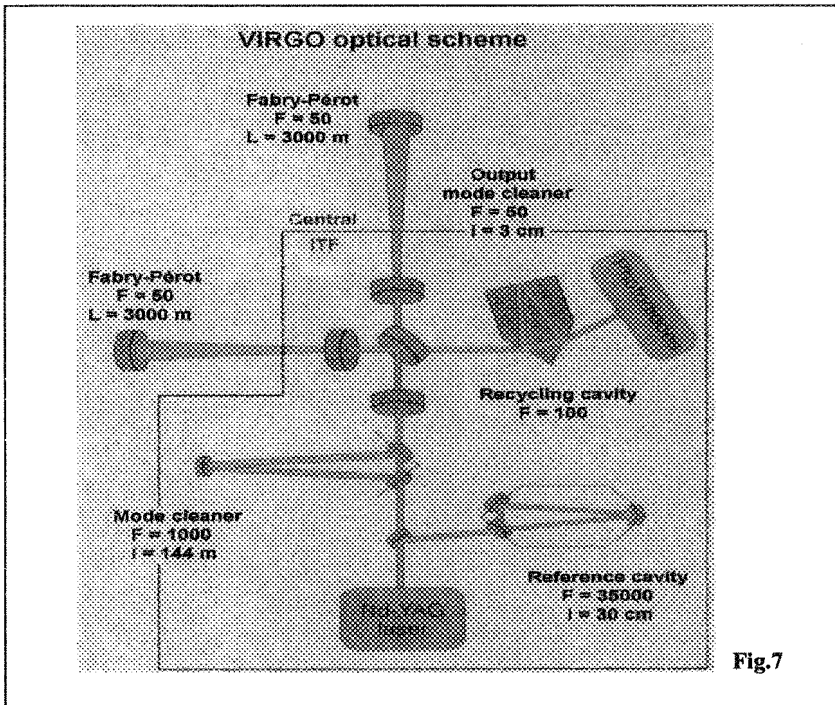


Fig.7

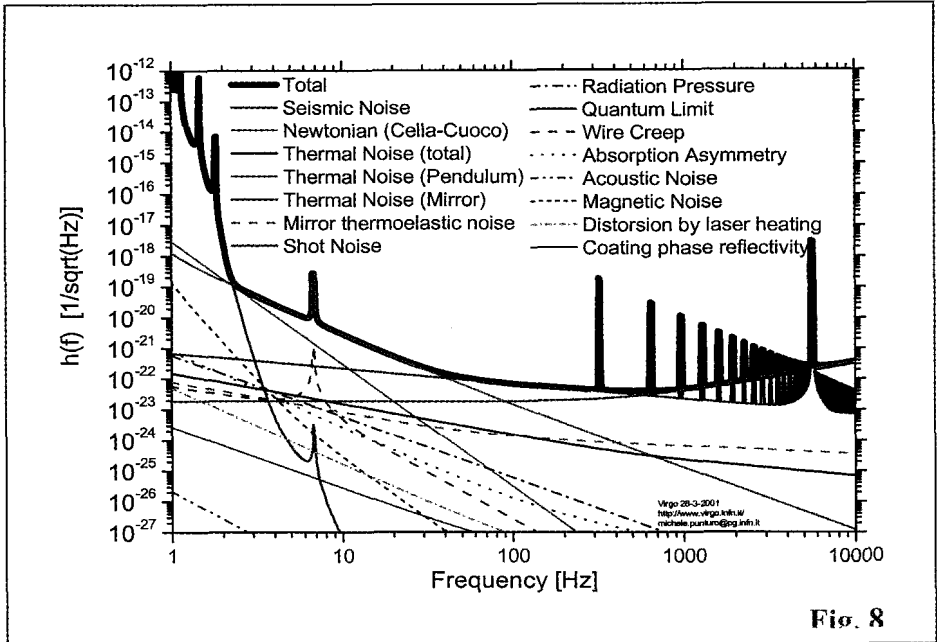


Fig. 8

The interferometric detector dominant noises.

Main contributions are shown in fig. 8 :

Seismic noise¹³: It is due to the continuous agitation of Earth crust due both to man and natural activity. If not attenuated it may give contributions as large as $\sim 10^{10}$ than GW signal.

Thermal noise¹⁴: Is created by the thermal agitation of atoms composing mirror substrate and his wire suspension. The thermal stockastic force is created by the materials internal friction, hence for having low thermal noise monocrystal mirror and mirror suspension wires are needed.

Shot noise: Is due to the granular nature of photons who is creating a phase fluctuation $\Delta\phi = N^{-1/2}$, where N is photon number. This noise is reduced increasing laser power.

Radiation Pressure noise: In FP cavities about 100 KW are stored; the photon number fluctuations produce a fluctuating force on the mirrors $\Delta f = Fd(N^{1/2}h\nu/c)/dt$, (where F is the cavity finesse and ν_l the laser frequency); this force produces a mirror position fluctuation.

Quantum Noise: represents the precision limit for mass M position measurement in a time t at the observing frequency ν ; it is obtained by minimizing the equivalent displacements due both to shot noise and radiation pressure noise. From this operation it follows the optimal laser power as function of M and ν .

Newtonian noise: Is produced by newtonian fluctuating force due to the seismic movement of Earth masses close to the test masses. Also wind is producing Newtonian noise. The Earth Newtonian noise can be reduced by putting a grid of seismometers around the detector and by reconstructing the produced noise.

The Laser and the frequency stabilization requirements

The laser system (see Fig. 9) is a 20 W ring with cristal Nd: YVO₄; this power unit is Injection-Locked to a 1W Monolithic YAG master prestabilized to a 30 cm triangular Ultra Low Expansion reference cavity. The prestabilization can reach 10^{-4} Hz/Hz^{0.5}@50 Hz. Due to the unavoidable storage time mismatch of the two 3km cavities, for reducing laser frequency noise effects, it is necessary to stabilize the laser by using as a frequency reference the 3 km cavities common mode. This allows to reach the frequency fluctuations specifications (10^{-6} Hz/Hz^{0.5}@10 Hz), needed for reaching the design sensitivity

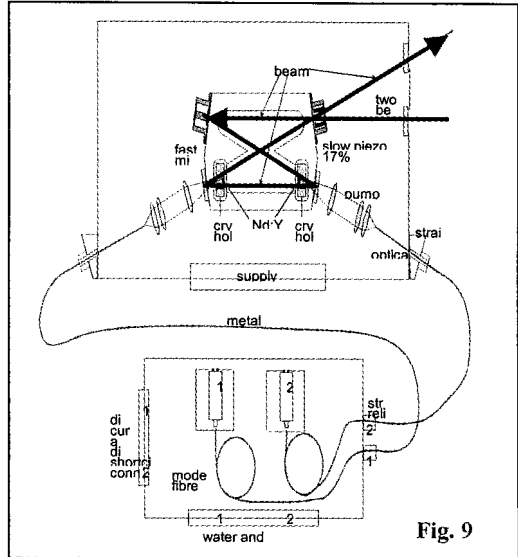


Fig. 9

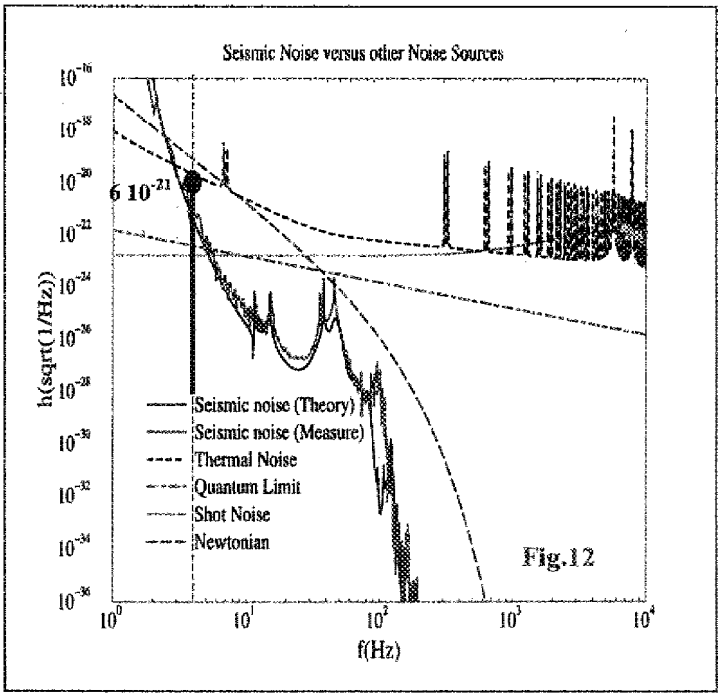
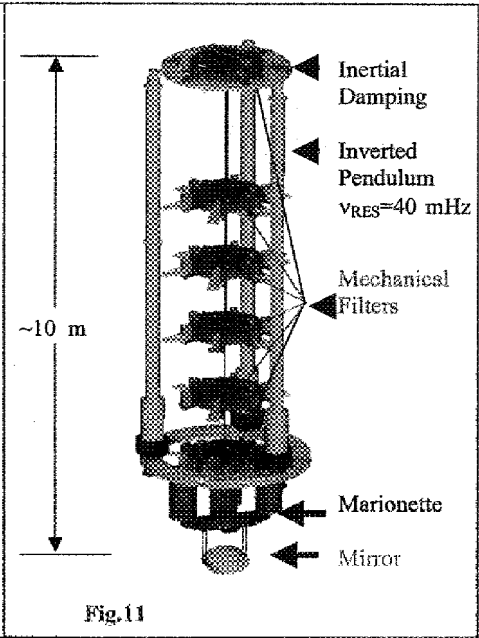
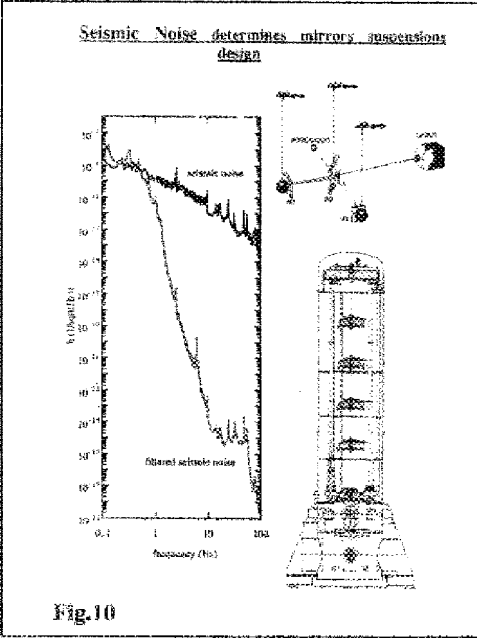
The Virgo Superattenuators and the Ierarchical control

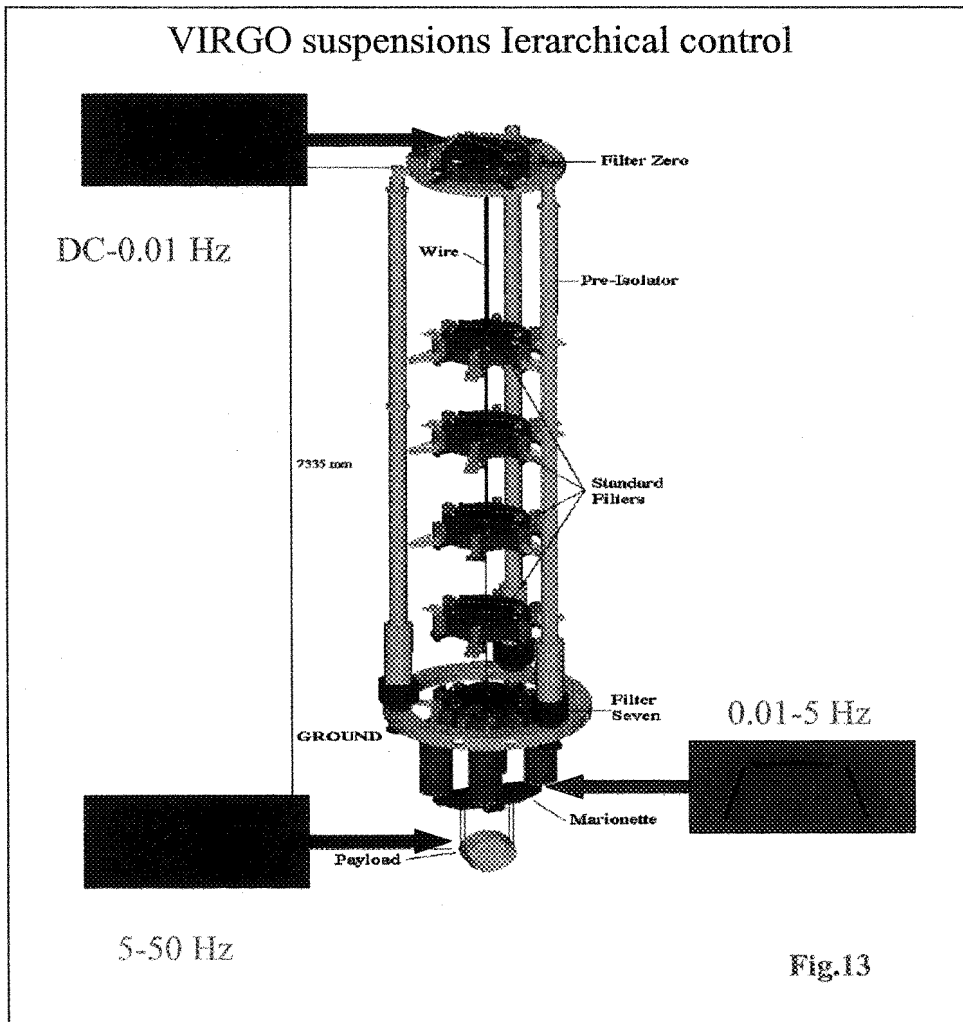
It is very important to underline the extremely high level of technology for Virgo design and specifications; Virgo mirror suspensions, called Superattenuators (SA), are unique and kill seismic noise in such a way to cross thermal noise at 4 Hz. The seismic performances are so good because every mechanical filter of SA isolate the rigid body in 6 dimensions, 3 translations and 3 rotations; this is the key to extreme seismic isolation i.e. for every mechanical filter there are not un-isolated degrees of freedom who may leave noise to go through.

In Fig. 10 the required specifications and in Fig. 11 the schematic diagram are shown. The inverted pendulum supports the inertial table actively isolated by means of 4 accelerometers, 3 on the horizontal plane and one in the vertical direction. This table supports the chain of mechanical filters together with marionette and mirror.

We have measured the upper limit of SA isolation at 4 Hz ; the value(see Fig. 12) perfectly stands on the attenuation transfer function(TF) obtained by measuring SA attenuation stage by stage and then multiplying the TF so obtained. SA structure allows to implement a very efficient mirror control; infact we may keep un-interrupted locking even in presence of large tidal SA displacement by distributing locking control signal at different levels of SA, as shown in Fig. 13.

With by the jerarchical control we obtain an optimal dynamicswise system; infact with SA the contro system should not introduce noise down to 4 Hz.

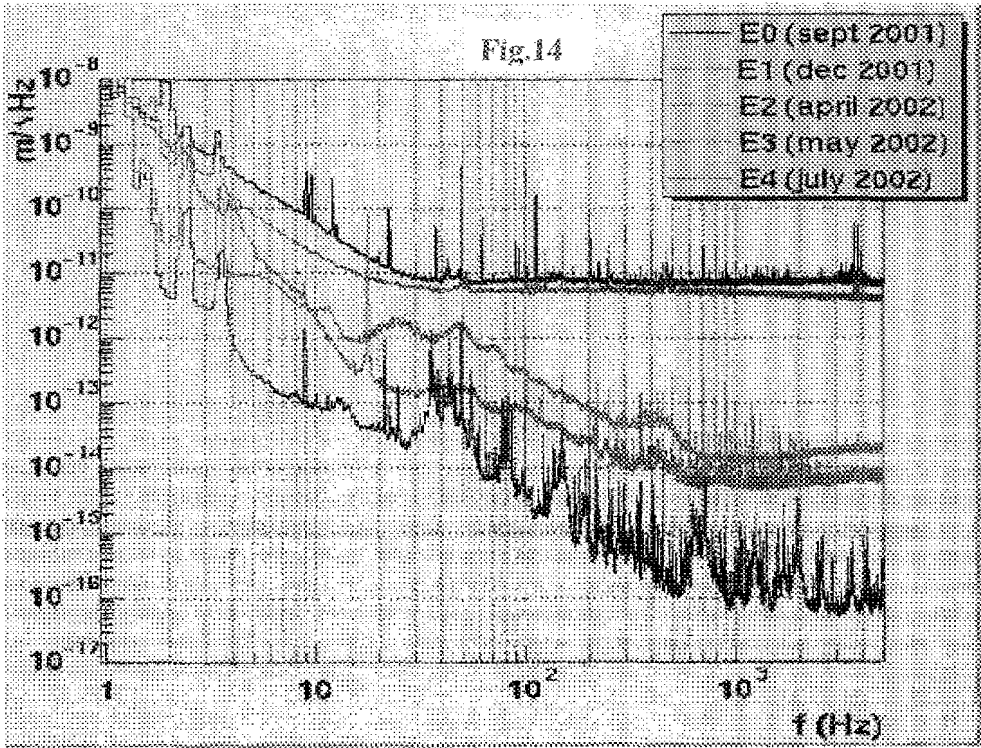




Results from the Central Interferometer (CITF) Commissioning

In the CITF operation the north and west input mirrors were used to create a short Michelson interferometer (see interferometer inside green part of Fig.7): in the latest runs also the recycling mirror was used.

Results from the CITF operation are shown in Fig. 14, and expressed in $\text{meter}/\text{Hz}^{-1/2}$. Central Interferometer operation ended successfully in July 2002 and the milestone required by INFN and CNRS was fulfilled.



Virgo Upgrading to 3km

Starting on september 2002 till october 2003 the following upgradings to Virgo were performed:

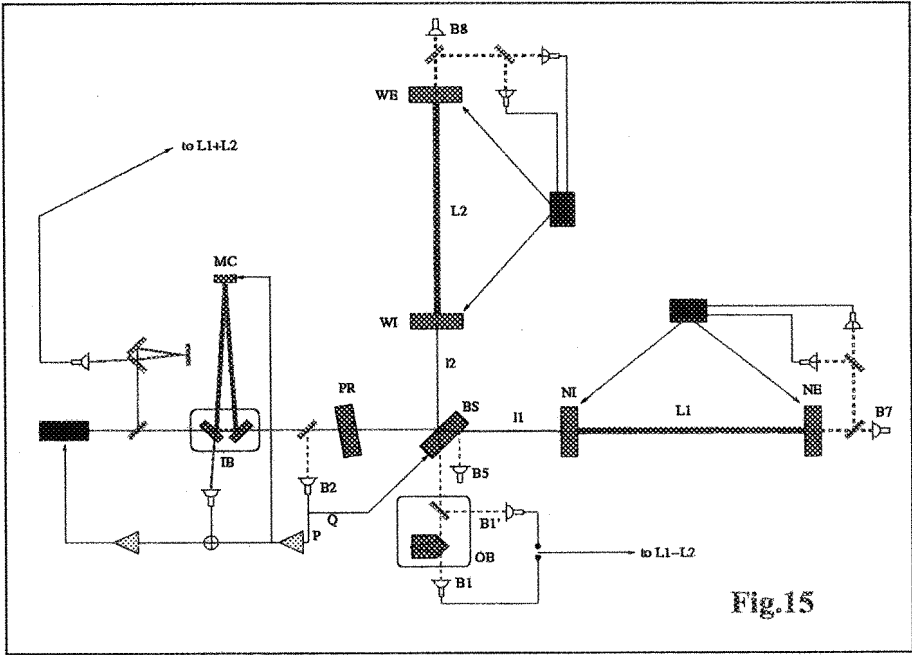
- 1) Completion of vacuum.
- 2) Mounting Nord and West end Superattenuators.
- 3) Mounting of high quality mirrors.
- 4) New Mode-Cleaner Mirror suspension.
- 5) More performant local controls.
- 6) More performant DSP for suspension control.

In July 2003 the upgradings ended and the 23 July 2003 the Virgo inauguration was performed. In september 2003 Virgo 3km Commissioning Started and the recombined 3+3 km cavities were operated (see diagram in fig. 15 and note the misaligned power recycling mirror).

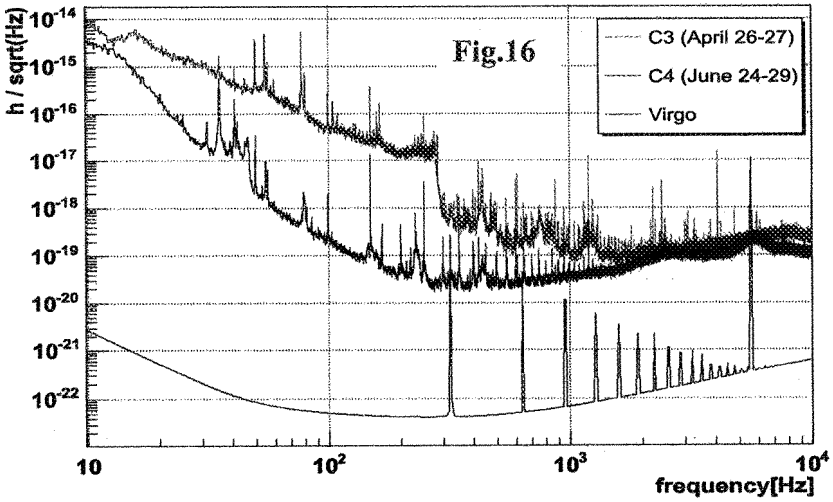
During these runs, C2 and C3, the longer was uninterrupted 28 hours, we had the following running conditions:

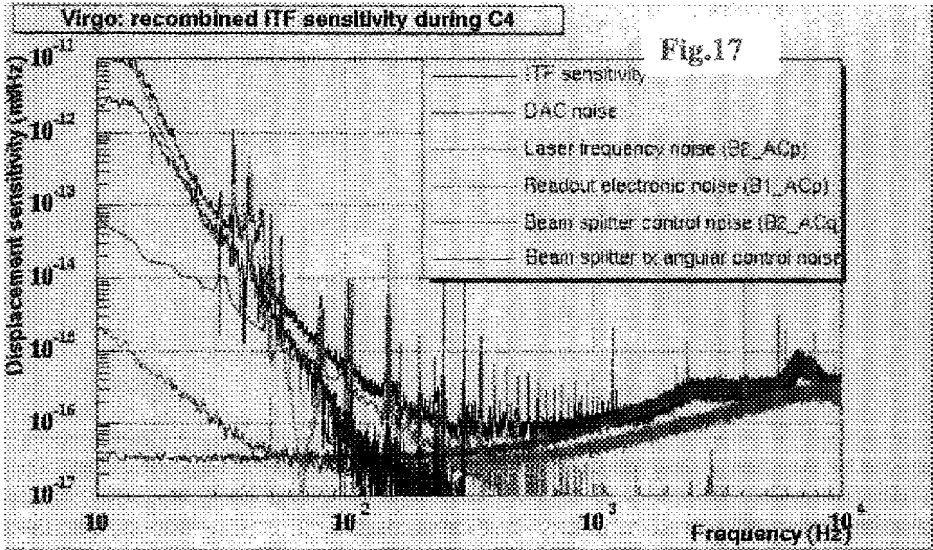
- 1) Laser frequency stabilized on the 3 km cavities common mode.
- 2) Cavities mirror were automatically aligned by using the (0,1) or (1,0) modes excitation.
- 3) The output mode cleaner, on the detection bench, needed for increasing black fringe contrast, was in operation.

In Fig. 16 results from these runs are presented and in Fig. 17 the principal contributions to recombined ITF noise are shown.



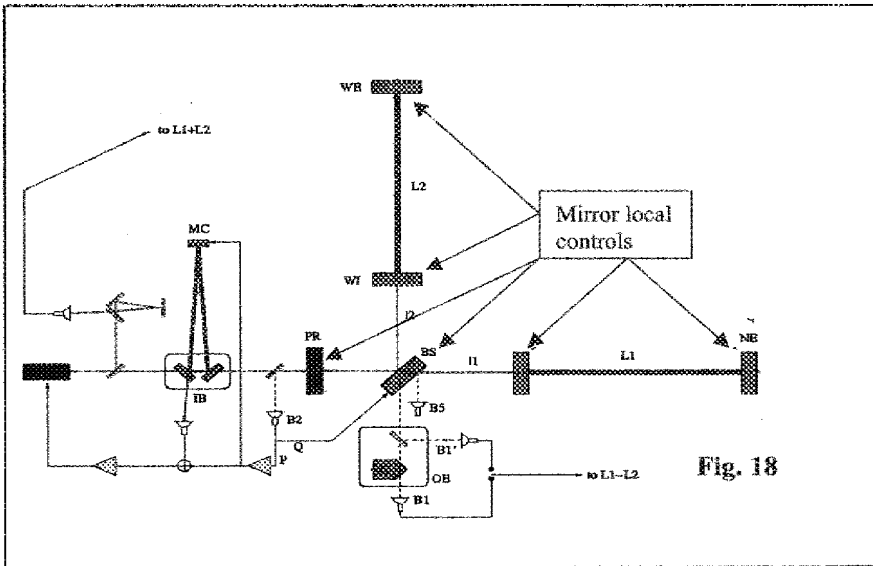
sensitivity

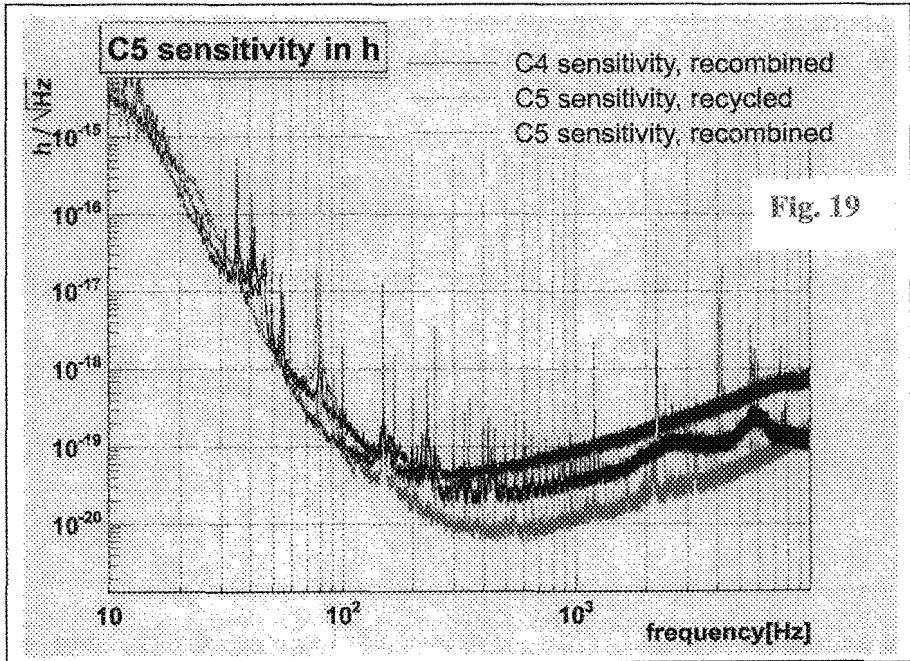




From the operation of recombined ITF and from the first attempt of recycling locking, we realized that the need of a Faraday isolator in the injection system

In September 2004 we started the recycled operation of Virgo; the Power Recycling mirror was aligned and the mirrors were aligned only with the local controls and not with the automatic alignment system (see Fig. 18), being the latter not yet ready for the recycled ITF. In Fig. 19 the sensitivities of C4 and of C5 both recombined and recycled, are shown.





Close future program

The main changes we have to perform during the first half 2005 are:

- 1) New injection bench equipped with Faraday isolator.
- 2) Change of mode cleaner mirror, being it too contaminated.
- 3) Substitution of power recycling curve-flat mirror with a flat-flat mirror.

After this changes are performed we can start to dig deeply into the noise hoping to reach the design sensitivity before end 2005.

References

- (1) -A.Einstein, Sitz. Ber. Kon.Preus. Ak. Wiss, 688(1916); id. 154(1918)
- (2) -C.W.Misner, K.S.Thorne, J.Wheeler, 1973, "Gravitation" (W.H.Freeman Eds.), S.Francisco.
-K.S.Thorne, 1987, "Gravitational radiation" in "300 years of gravitation" (Edited by S.W.Hawking and W.Israel, Cambridge University Press), New York (9) 330-458.
- (3) -R.A.Hulse and J.H. Taylor, *Astrophys. J. Lett.* 195, 151 (1975)-H.V.Shapiro, S.A.Teukolsky, 1984, "The physics of compact objects" (J.Wiley and Sons, Eds.), New York.

- (4)-Danilo Babusci (Frascati), Massimo Giovannini (Lausanne U.) "SENSITIVITY OF A VIRGO PAIR TO RELIC GW BACKGROUNDS". Aug 2000. 25pp. **Class.Quant.Grav.**17:2621-2633,2000
- Michele Maggiore "GRAVITATIONAL WAVE EXPERIMENTS AND EARLY UNIVERSE COSMOLOGY" **Phys.Rept.**331:283-367,2000
- (5)-J. Weber, **Phys. Rev.**117,306 (1960)
- J. Weber, **Phys. Rev. Lett.** 22,1302(1969)
- (6) -E. Coccia, 1995 "Resonant-mass gravitational wave detectors" in "*14th International Conference on General Relativity and Gravitational Physics*, Florence, August 6-12, 1995"
- (7) -P. Astone et al. "Recent results of Nautilus" in *Gravitational Waves*, third Amaldi Conference, Pasadena Ca. 12-16 July 1999 , AIP Conference Proceedings # 523, Melville, New York).
- (8) -M. Cerdonio et al. "Status Report of the Gravitational Wave Detector AURIGA" in "*Gravitational Waves*, third Amaldi Conference, Pasadena Ca. 12-16 July 1999 , AIP Conference Proceedings # 523, Melville, New York).
- (9) -D. Blair et al. "Niobe: improved noise temperature and Background Noise Suppression" in *Gravitational Waves*, third Amaldi Conference, Pasadena Ca. 12-16 July 1999 , AIP Conference Proceedings # 523, Melville, New York).
- (10) - J.J. Johnson et al. in *Gravitational Wave Experiments*, Proceedings of the First Edoardo Amaldi Conference, Frascati 1994,(World Scientific, Singapore, 1995)"
- (11) - A. Giazotto "Interferometric Detection of of Gravitational Waves", **Physics Rept**, 182, 6, 1989.
- (12) - J.Y.Vinet, B.Meers, C.N.Man, A.Brillet, **Phys. Rev. D** 38 (1988) 433.
- A.Brillet, *Ann. de Phys.* 10 (1985) 219.
- (13) - R. Del Fabbro et al., 1988,Phys. Lett. A132,237
- S.Braccini et al., 1997, "*Design of the superattenuators for the VIRGO construction*" VIRGO Internal Report (VIR-TRE-PIS-4600-134).
- (14) - H.B.Callen, R.F.Greene, **Phys. Rev.** 86 (1952) 702.